Published in final edited form as:
Eur J Neurosci. 2008 June ; 27(12): 3205–3215. doi:10.1111/j.1460-9568.2008.06307.x.

Age-related changes in dopamine transporters and accumulation of 3-nitrotyrosine in rhesus monkey midbrain dopamine neurons: Relevance in selective neuronal vulnerability to degeneration

N. M. Kanaan[1], **J. H. Kordower**[1], and **T. J. Collier**[2]

[1]Department of Neurological Sciences, Rush University Medical Center, Chicago, IL, USA

[2]Department of Neurology, University of Cincinnati, PO Box 670525, 265 Albert Sabin Way, Cincinnati, OH 45267, USA

Abstract

Aging is the strongest risk factor for developing Parkinson's disease (PD). There is a preferential loss of dopamine (DA) neurons in the ventral tier of the substantia nigra (vtSN) compared to the dorsal tier and ventral tegmental area (VTA) in PD. Examining age-related and region-specific differences in DA neurons represents a means of identifying factors potentially involved in vulnerability or resistance to degeneration. Nitrative stress is among the factors potentially underlying DA neuron degeneration. We studied the relationship between 3-nitrotyrosine (3NT; a marker of nitrative damage) and DA transporters [DA transporter (DAT) and vesicular monoamine transporter-2 (VMAT)] during aging in DA subregions of rhesus monkeys. The percentage of DA neurons containing 3NT increased significantly only in the vtSN with advancing age, and the vtSN had a greater percentage of 3NT-positive neurons when compared to the VTA. The relationship between 3NT and DA transporters was determined by measuring fluorescence intensity of 3NT, DAT and VMAT staining. 3NT intensity increased with advancing age in the vtSN. Increased DAT, VMAT and DAT/VMAT ratios were associated with increased 3NT in individual DA neurons. These results suggest nitrative damage accumulates in midbrain DA neurons with advancing age, an effect exacerbated in the vulnerable vtSN. The capacity of a DA neuron to accumulate more cytosolic DA, as inferred from DA transporter expression, is related to accumulation of nitrative damage. These findings are consistent with a role for aging-related accrual of nitrative damage in the selective vulnerability of vtSN neurons to degeneration in PD.

Keywords

nitration; nonhuman primate; Parkinson's disease; substantia nigra; ventral tegmental area

Correspondence: Dr T. J. Collier, as above. timothy.collier@uc.edu.

Supplementary material

The following supplementary material may be found on http://www.blackwell-synergy.com

Fig. S1. The 3NT primary antibody is specific for nitrated tyrosine.

Table S1. Estimated $3NT^+$ cell numbers and $3NT^+$ cell volumes, optical density of 3NT-ir, DAT-ir, VMAT-ir, and DAT/VMAT ratios in the vtSN, dtSN, and VTA of young, middle-age, and old-age monkeys.

Table S2. DAT, VMAT, and DAT/VMAT ratios are predictors of 3NT levels in midbrain DA neurons.

Please note: Blackwell Publishing are not responsible for the content or functionality of any supplementary materials supplied by the authors. Any queries (other than missing material) should be directed to the correspondence author for the article.

Introduction

Accumulating evidence suggests age-related changes in dopamine (DA) neurons are related to pathological changes associated with Parkinson's disease (PD) (e.g. Chu and Kordower, 2007, Kanaan *et al.*, 2007). In PD, DA neuron degeneration follows a region-specific pattern in which DA neurons in the ventral tier of the substantia nigra (vtSN) are substantially more vulnerable than dorsal tier (dtSN) and ventral tegmental area (VTA) DA neurons (Gibb & Lees, 1991; Damier *et al.*, 1999). Thus, examining age-related changes within specific DA subregions represents a powerful strategy for further understanding mechanisms underlying DA neuron degeneration in PD.

Among factors potentially involved in the pathogenesis of PD is oxygen and nitrogen free radical-mediated cellular damage (Jenner, 2003; Reynolds *et al.*, 2007). Oxidative and nitrative stress are measured using markers for the modifications which free radicals make to macromolecules (e.g. tyrosine nitration). Tyrosine nitration can occur through multiple pathways with nitric oxide providing the source of nitrogen (Ischiropoulos, 2003). Peroxynitrite, a reactive nitrogen species made from the reaction between superoxide anions and nitric oxide (Torreilles *et al.*, 1999; Salvemini *et al.*, 2006), can generate 3-nitrotyrosine (3NT) residues within proteins. Free radical damage can interfere with macromolecule function and promote protein aggregation, which may precipitate cellular dysfunction and degeneration (Beckman & Koppenol, 1996; Squier, 2001; Reynolds *et al.*, 2007).

Free radical damage is normally high in the human substantia nigra (SN; Floor & Wetzel, 1998), is increased in the SN of PD cases (Alam *et al.*, 1997a,b; Duda *et al.*, 2000; Giasson *et al.*, 2000) and is increased in numerous brain regions during aging (Uttenthal *et al.*, 1998; Sloane *et al.*, 1999; Shin *et al.*, 2002; Del Moral *et al.*, 2004). However, the age-related accumulation of nitrative damage in specific midbrain DA subregions remains unknown.

DA taken back into DA neurons by dopamine transporters (DAT) represents a source of free radicals via metabolism and/or autooxidation of cytosolic DA (Asanuma *et al.*, 2004; Hald & Lotharius, 2005). Subsequently, DA neurons can protect against DA-derived free radicals by sequestering cytosolic DA into synaptic vesicles with vesicular monoamine transporter-2 (VMAT). Thus, neurons expressing more DAT, less VMAT and/or higher DAT/VMAT ratios are potentially exposed to more DA-derived free radicals and cellular damage, rendering them more susceptible to degeneration (Haber *et al.*, 1995; Miller *et al.*, 1999; Gonzalez-Hernandez *et al.*, 2004; Liang *et al.*, 2004). The relationship between DA transporters and nitrative stress has not been examined in midbrain DA subregions.

The association between aging and PD suggests factors involved in the development of PD should accumulate with advancing age and in region-specific patterns consistent with known vulnerability or resistance to degeneration. We hypothesized that vulnerable vtSN DA neurons would accumulate more nitrative damage during aging, which would be associated with a greater capacity to accumulate cytosolic DA. Confirming our hypothesis, an age-related increase in nitration occurred specifically in the vulnerable vtSN and greater nitrative damage was associated with higher DAT, VMAT and DAT/VMAT ratios in individual DA neurons. These data suggest age-related nitrative damage and levels of DAT and VMAT in midbrain DA neurons are important factors in differential vulnerability of DA neurons to degeneration.

Materials and methods

Animals and tissue collection

Tissues from the same young (9–10 years, $n = 3$), middle-aged (14–17 years, $n = 6$) and old-aged (22–29 years, $n = 5$) naïve rhesus monkeys described in Kanaan *et al.* (2007) were used in the current study. The Institutional Animal Care and Use Committees of Rush University Medical Center and the Biological Research Laboratory at the University of Illinois at Chicago approved all experimental protocols. All laws and regulations outlined in the National Institutes of Health, United States Public Health Service Guide for the Care and Use of Laboratory Animals were adhered to during the project. All animals were killed using an overdose of pentobarbital (50 mg/kg, i.v.) followed by transcardial perfusion with physiological saline. Tissue was collected and prepared for immunohistochemistry and immunofluorescence as described previously (Kanaan *et al.*, 2007).

Antibodies

The following primary antibodies were used for immunohistochemistry and immunofluorescence: rabbit anti-VMAT2 (Chemicon; AB1767), rat anti-DAT (Chemicon, MAB369), rabbit anti-3-nitrotyrosine (Upstate; 06–284) and mouse anti-tyrosine hydroxylase (TH; Chemicon; MAB318). The secondary antibodies included: biotinylated goat anti-rabbit IgG (H + L; Vector; BA-1000), biotinylated goat anti-rat IgG (H + L; Vector; BA-9400), Alexa Fluor® 488-conjugated streptavidin (Molecular Probes; S-11223, lot 43500A) and Alexa Fluor® 647-conjugated goat anti-rabbit IgG (H + L; Molecular Probes; A-21244), AffiniPure Fab fragment goat anti-rabbit IgG (H + L; JacksonImmunoResearch; 111-007-003) and biotinylated goat antimouse IgG (H + L; Chemicon; AB124B). The specificity of the 3NT primary antibody was confirmed using preadsorption controls (Supplementary material, Fig. S1). Preadsorbing the 3NT antibody with 12 mM 3NT (3-nitro-L-tyrosine; Cayman Chemical; 89540) prior to use in our protocols blocked all staining (supplementary Fig. S1B). The specificity of the 3NT antibody was further confirmed by preadsorbing against 12 mM L-tyrosine (Sigma; T3754), which did not block staining (supplementary Fig. S1C). All of the controls worked as expected and confirmed the specificity of the 3NT primary antibody.

3NT immunohistochemistry

Following a similar protocol to those previously published (Kanaan *et al.*, 2006, 2007) a 1-in-12 series of tissue was processed for 3NT or TH immunohistochemistry. Briefly, the tissue sections were incubated in 0.6% H_2O_2 to quench endogenous peroxidase activity and then incubated in blocking solution. Then sections were incubated in either rabbit anti-3NT (1 : 400) or mouse anti-TH antibody (1 : 4000). Sections were incubated in the secondary antibody solution containing either biotinylated goat anti-rabbit or biotinylated goat anti-mouse (both at 1 : 400), and then in avidin–biotin complex solution. Both stains were developed using 3,3-diaminobenzidine tetrahydrochloride (Sigma; D5637) enhanced with 2% nickel ammonium sulfate (Fisher; N48-500). Sections were mounted on microscope slides, dehydrated through graded ethanol solutions, cleared in xylenes and coverslipped. All sections were processed for immunohistochemistry simultaneously to reduced staining variability.

Unbiased stereological cell counting and cell volume

The number of 3NT-positive$^+$ cells was estimated in the vtSN, dtSN and VTA of young, middle-aged and old-aged monkeys using the optical fractionator stereological cell counting probe as previously described (Kanaan *et al.*, 2007). The vtSN, dtSN and VTA were outlined at low magnification (1.25×). The counting frame size was 100 × 75 μm and the

sampling grid size was 700 × 450 μm for the vtSN, 120 × 152 μm for the dtSN and 331 × 365 μm for the VTA. The Gundersen method for calculating the coefficient of error was used to estimate the accuracy of the optical fractionator results (West & Gundersen, 1990; Gundersen *et al.*, 1999). The coefficients of error were between 0.14 and 0.07. The volume of $3NT^+$ cells was measured using the nucleator probe as previously described (Kanaan *et al.*, 2007).

Triple-label immunofluorescence

To determine relative fluorescence intensity of DAT, VMAT and 3NT staining in individual midbrain DA neurons, a 1-in-24 series of tissue was stained using triple-label immunofluorescence for DAT, VMAT and 3NT following a similar protocol as previously described (Kanaan *et al.*, 2007). The tissue was incubated in 0.6% H_2O_2 to quench endogenous peroxidase, then in blocking solution, followed by the DAT primary antibody solution (1 : 50). The following day, sections were incubated in biotinylated goat anti-rat antibody and then incubated in Alexa Fluor® 488-conjugated streptavidin. Then the remaining open binding sites for biotin and avidin were blocked using an avidin–biotin blocking kit (Vector; SP-2001), which was followed by incubation in the 3NT primary antibody (1 : 300). The next day, sections were incubated in biotinylated goat anti-rabbit secondary antibody and then in avidin–biotin complex solution. A fluorescent tyramide derivative was used to develop the stain (Alexa Fluor® 555 tyramide, diluted 1 : 150 in amplification buffer made according to the manufacturer's instructions; Molecular Probes; T30954). As 3NT and VMAT primary antibodies were made in rabbits, the appropriate blocking steps were taken. The tissues were incubated in 4% rabbit serum and then in an excess concentration of goat anti-rabbit Fab fragment (1 : 65). Then tissues were incubated in VMAT primary antibody (1 : 200). The following day, sections were incubated in Alexa Fluor® 647-conjugated goat anti-rabbit secondary antibody (1 : 200). Then the sections were mounted on microscope slides and autofluorescence was blocked using the autofluorescence eliminator reagent (Chemicon; 2160, lot 0612047871) as previously described (Kanaan *et al.*, 2007). After autofluorescence blocking, the sections were coverslipped using Gel/Mount (Biomeda; M01, lot 21433). All sections were stained simultaneously to reduced variability.

The effectiveness of the avidin–biotin blocking step was confirmed empirically (data not shown). Sections were processed for DAT immunofluorescence, then the avidin–biotin blocking step was performed, and then the sections were incubated in biotinylated goat anti-rabbit secondary antibody, avidin–biotin complex solution and Alexa Fluor® 555 tyramide substrate as described above. This procedure produced the expected DAT pattern of immunofluorescence and Alexa Fluor® 555 fluorescence was not detected, which confirmed the effectiveness of the blocking step. Blocking for two primary antibodies from the same host species was confirmed empirically (data not shown). Tissue sections were incubated in 3NT primary antibody, biotinylated goat anti-rabbit secondary, avidin–biotin complex solution, Alexa Fluor® 555 tyramide substrate solution, 4% rabbit serum, goat anti-rabbit Fab fragment, VMAT primary antibody and Alexa Fluor® 647-conjugated goat anti-rabbit secondary antibody. This procedure produced a pattern of 3NT labeling that was similar to our 3NT immunohistochemistry results (neurons and glial cells), and Alexa Fluor® 647 fluorescence only labeled neurons in the typical pattern of catecholamine immunolabeling (data not shown). Importantly, there was not 100% co-localization. The patterns of 3NT and VMAT immunoreactivity were different within individual neurons and 3NT labeling was present in non-catecholamine neurons and glial cells (which were negative for VMAT). These results confirm that blocking for two primary antibodies made in the same host species was effective.

Quantitative image analysis: fluorescence intensity measurement

Relative fluorescence intensity of DAT, VMAT and 3NT immunostaining within individual DA neurons was quantified using similar methods to those previously described (Kanaan *et al.*, 2007). DAT immunofluorescence was detected using excitation of 488 nm and an emission filter of 505–525 nm. 3NT immunofluorescence was detected using excitation of 543 nm and an emission filter of 560–600. VMAT immunofluorescence was detected using excitation of 633 nm and an emission filter of 660-infared. Autofluorescence did not contribute to the fluorescence as it was effectively blocked in this and control experiments (as described above).

Numerous images covering each region (vtSN, dtSN and VTA) within sections throughout the rostral–caudal extent of the SN were acquired at 30× magnification and used for measuring fluorescence intensity. Each image contained multiple neurons triple-labeled with DAT, VMAT and 3NT. The average number of triple-labeled neurons per animal that were used for analysis was 111 in the vtSN, 52 in the dtSN and 72 in the VTA. All confocal settings were maintained between each animal and the sequential scan mode was used to ensure that crossover between fluorophores did not occur. Average pixel intensity was measured using ImageJ version 1.36b software (National Institutes of Health, Bethesda, MD, USA). This analysis measures the mean pixel intensity ranging from 0 (black) to 4095 (white). Background levels were determined in areas of the cerebral peduncle and were subtracted from each measurement made in the vtSN, dtSN and VTA. Only triple-labeled neurons (DAT^+, $VMAT^+$ and $3NT^+$) were used in these analyses. A single intensity value for each region in each animal was calculated by taking the average of the mean pixel intensity for all individual neurons. Individual neuron intensity values were used only in regression analyses to determine whether DAT intensity, VMAT intensity or DAT/VMAT intensity ratios predicted 3NT intensity.

Statistics

Nonparametric statistical tests were used to analyze the data (Kanaan *et al.*, 2007). The Kruskal–Wallis one-way analysis of variance on ranks test was utilized to determine differences between age groups. The Spearman rank correlation was used for correlations with chronological age. To determine whether the intensity of DAT, VMAT or DAT/VMAT in individual neurons predicted the level of 3NT staining, linear regression model analyses were performed. Comparisons between the three DA subregions within each age group were performed using the Friedman repeated-measures analysis of variance on ranks test. When overall significance was reached, Dunn's method was used for *post hoc* comparisons. $P = 0.05$ was considered statistically significant. All statistics were calculated using SigmaStat version 3.0.1 software (SPSS, Chicago, IL, USA).

Results

General observations

DAT and VMAT immunoreactivity followed the normal distribution of DA neurons and fibers. 3NT immunoreactivity was consistent with labeling in both neurons and glial cells. As described above, all control sections confirmed the specificity of the secondary and primary antibodies, and little background was detected for all stains. Supplementary Table S1 provides the mean (± SEM) of cell count, cell volume and fluorescence intensity data. Due to the similarities in results of the two statistical tests used to analyze differences with advancing age (analysis of variance on ranks for age group comparisons and correlations for association with chronological age), only the results of age group comparisons are presented to reduce redundancy.

The percentage of DA neurons containing 3NT increased with advancing age in the vtSN

To determine the effects of age on the regional distribution of nitrative damage (3NT immunoreactivity) in the midbrain, the number of $3NT^+$ neurons in the vtSN, dtSN and VTA of young, middle-aged and old animals was quantified using stereological cell counting methods. While colocalization studies were not performed in this analysis, the presence of neuromelamin and the colocalization between 3NT, VMAT and DAT confirmed the dopaminergic nature of these cells. Moreover, the cell volume (μm^3) of $3NT^+$ neurons in the DA subregions (supplementary Table S1) were similar to the volumes of TH^+ neurons previously reported (Kanaan *et al.*, 2007). When age groups (young vs. middle-aged vs. old-aged) were compared in each subregion, there was not a significant difference in the number of $3NT^+$ neurons in any of the midbrain subregions ($P > 0.05$; Fig. 1A). However, a trend toward increased numbers of $3NT^+$ neurons was seen in the vtSN ($P = 0.098$). In old animals, the cell number density ($cells/mm^3$) of $3NT^+$ neurons was significantly greater in the vtSN than in the VTA ($P = 0.05$; Fig. 1A). Thus, in aged animals the vtSN had more $3NT^+$ neurons than the VTA, and aging was associated with a mild nonsignificant increase in the number of $3NT^+$ neurons.

Based on these observations, we expressed the number of $3NT^+$ neurons as a percentage of TH^+ neurons for each subregion (previously reported for the same animals used here; Kanaan *et al.*, 2007) to further delineate the relationship between $3NT^+$ and DA neurons within different midbrain subregions. This allowed us to determine the age-related and region-specific changes in the number of DA neurons containing 3NT. In the vtSN, the percentage was significantly greater in aged animals than in young animals ($P < 0.05$; Fig. 1B). In contrast, in the dtSN and VTA the percentage was not significantly different between age groups ($P > 0.05$; Fig. 1B). In all three age groups, the vtSN had the highest percentage of $3NT^+$ neurons ($P < 0.05$ vs. VTA; Fig. 1B). Figure 2 illustrates the age-related increase in the proportion of TH^+ neurons containing 3NT in the vtSN and VTA (compare A and B to E and F, and C and D to G and H). Also, the greater proportion of TH^+ neurons containing 3NT in the vtSN than in the VTA is illustrated in Fig. 2. Note that the change in the percentage was mostly due to the age-related reduction in TH^+ neurons as the numbers of $3NT^+$ neurons were not significantly altered with advancing age (Kanaan *et al.*, 2007; see Discussion). Thus, when the number of $3NT^+$ neurons was expressed as a percentage of TH^+ neurons, aging was associated with an increase in DA neurons that contain 3NT specifically in the vtSN, and the vtSN region had a greater percentage than the VTA in all age groups.

Intensity of 3NT immunofluorescence was increased specifically in the vtSN with advancing age

To further study the age-related and region-specific accumulation of nitrative damage, the fluorescence intensity of 3NT immunofluorescence was quantified. In the vtSN, aged animals had significantly greater levels of 3NT immunofluorescence when compared to young (+110%) and middle-aged (+116%) animals ($P < 0.05$; Fig. 3A). In contrast, in the dtSN and VTA, young, middle-aged and old animals had similar levels of 3NT ($P > 0.05$; Fig. 3A). The robust increase in 3NT immunofluorescence in vtSN neurons in aged animals is readily appreciable in Fig. 4 (compare A to C). In young animals, $3NT^+$ neurons in the three DA subregions had similar levels of 3NT immunofluorescence ($P > 0.05$; Fig. 3A; compare Fig. 4A to E). In middle-aged animals, the neurons in the VTA had greater levels of 3NT than those in the dtSN (+178%; $P < 0.05$; Fig. 3A). In aged animals, the level of 3NT in the vtSN DA neurons was significantly greater than the level in dtSN neurons (+172%; $P < 0.05$; Fig. 3A; compare Fig. 4C to G). Thus, aging was associated with increasing levels of 3NT immunofluorescence, specifically in vtSN DA neurons.

Intensity of DAT immunofluorescence was reduced with increasing age and was greatest in the vtSN

To determine the age-related and region-specific changes in DAT we measured the fluorescence intensity of DAT immunofluorescence. In the vtSN and VTA, the intensity of DAT was similar between young, middle-aged and old animals ($P > 0.05$; Fig. 3B), although modest declines were apparent. In the dtSN of middle-aged animals, the intensity of DAT was significantly greater than the DAT intensity in old-aged neurons ($P < 0.05$; Fig. 3B). In all three age groups, the vtSN had the highest level of DAT immunofluorescence, which was significantly different from the dtSN ($P < 0.05$; Fig. 3B, compare Fig. 5A to B and C to D). Thus, the vtSN DA neurons had the highest levels of DAT at all ages and, while DAT tends to decline with advancing age, this decrease was only significant in the dtSN.

Intensity of VMAT immunofluorescence was unchanged with age and greatest in the vtSN

To determine the age-related and region-specific changes in VMAT we measured the fluorescence intensity of VMAT. In the vtSN, dtSN and VTA, the intensity of VMAT immunofluorescence was similar between young, middle-aged and old animals ($P > 0.05$; compare Fig. 5A′ to C′ and B′ to D′). In young animals, the three subregions had similar levels of VMAT immunofluorescence ($P > 0.05$; Fig. 3C; compare Fig. 5A′ to B′). In middle-aged and old animals, VMAT intensity was greatest in the vtSN, statistically significantly greater than the dtSN ($P > 0.05$; Fig. 3C; compare Fig. 5C′ to D′). Thus, vtSN DA neurons had the highest levels of VMAT expression, and VMAT intensity did not change with advancing age.

DAT/VMAT intensity ratio was reduced with increasing age and greatest in the vtSN

The ratio of DAT intensity to VMAT intensity was calculated to determine whether there was an age-related and/or region-specific shift in DAT/VMAT ratios. In addition, DAT/VMAT ratios may act as a relative index for the capacity of a DA neuron to accumulate cytosolic DA (e.g. more DAT and less VMAT gives a higher DAT/VMAT ratio and increased capacity to accumulate cytosolic DA; Haber *et al.*, 1995; Miller *et al.*, 1999; Liang *et al.*, 2004; Gonzalez-Hernandez *et al.*, 2004). In the vtSN, the DAT/VMAT ratio was similar between young, middle-aged and old animals ($P > 0.05$; Fig. 3D). In the dtSN, the DAT/VMAT ratio was significantly greater in middle-aged animals than in old animals ($P < 0.05$; Fig. 3D). In the VTA, the DAT/VMAT ratio was similar between the three age groups but a decrease in the ratio approached statistical significance ($P = 0.055$; Fig. 3D). However, when correlation analyses were used, advancing chronological age was associated with significant reductions in DAT/VMAT ratios in all DA subregions ($P < 0.05$; data not shown). In young and middle-aged animals, the vtSN, dtSN and VTA neurons exhibited similar DAT/VMAT ratios; however, in aged animals the DAT/VMAT ratio in vtSN neurons was significantly greater than the DAT/VMAT ratio in dtSN neurons ($P < 0.05$; Fig. 3D). Given the lack of age-related changes in VMAT intensity, age-related reductions in DAT intensity were driving the reduction in the DAT/VMAT ratio. Additionally, linear regression analyses were performed between DAT and VMAT levels, and in all DA subregions of all age groups higher levels of DAT were correlated with higher levels of VMAT (data not shown). Thus, the DA neurons of the vtSN had the greatest DAT/VMAT ratio in aged animals, and aging was associated with reductions in the DAT/VMAT ratio because of reduced DAT intensity.

DAT, VMAT and the DAT/VMAT ratio predicted the level of 3NT immunofluorescence

The mean pixel intensity from individual triple-labeled neurons was evaluated using linear regression models to determine whether levels of DAT, VMAT, or DAT/VMAT ratios was predictive of 3NT fluorescence levels (supplementary Table S2). Each variable was entered

singly into a linear regression model with 3NT intensity as the dependent variable. DAT and VMAT levels were significant predictors of 3NT levels in all DA subregions of all age groups except the dtSN of young animals. DAT/VMAT ratios were significant predictors of 3NT immunofluorescence levels only in the vtSN of aged animals, the dtSN of middle-aged and old animals and the VTA of aged animals. Higher levels of DAT, VMAT and DAT/VMAT ratios were associated with higher levels of 3NT, as indicated by positive *R*-values for all of the linear regressions (supplementary Table S2).

The co-localization of 3NT in midbrain DA neurons (DAT^+ and $VMAT^+$) was confirmed using confocal microscopy (Fig. 6A–D). The majority of $3NT^+$ neurons in the vtSN, dtSN and VTA were also DAT^+ and $VMAT^+$, which confirms that the majority of $3NT^+$ neurons analyzed in the current study were DA neurons. Lastly, the relationships of DAT, VMAT and DAT/VMAT ratios to 3NT intensity are illustrated in the representative confocal microscopic images in Fig. 6E–H. Note that higher DAT, VMAT and DAT/VMAT ratios were associated with higher levels of 3NT. Thus, greater accumulation of 3NT in DA neurons was associated with higher levels of DAT, VMAT and, importantly, higher DAT/VMAT ratios (indicative of an increased capacity to accumulate cytosolic DA).

Discussion

This is the first report describing the regional distribution of $3NT^+$ neurons during normal aging in DA subregions of the nonhuman primate midbrain. Aging was associated with accumulation of 3NT in midbrain DA neurons and vulnerable vtSN DA neurons were susceptible to greater nitrative damage. In addition, this is the first report describing the relationship between DAT and VMAT levels and 3NT levels in DA neurons of specific midbrain subregions. Greater levels of nitrative damage was associated with a greater capacity to accumulate cytosolic DA, as indicated by levels of DA transporters.

We found 3NT-immunoreactive neuronal profiles in the midbrain of rhesus monkeys of all ages. These results are consistent with previous studies that detected 3NT immunoreactivity in young, adult and aged rats and nonhuman primates. $3NT^+$ neurons and glial cells have been found in the striatum, cerebral cortex, hippocampus, cerebellum and subcortical white matter (Uttenthal *et al.*, 1998; Sloane *et al.*, 1999; Chung *et al.*, 2002; Shin *et al.*, 2002; Del Moral *et al.*, 2004). It is noteworthy that some studies detected little or no 3NT immunoreactivity in adult rats and baboons (Ferrante *et al.*, 1999; Chung *et al.*, 2002; Shin *et al.*, 2002). Species differences and technical differences in 3NT immunohistochemistry protocols probably are among the factors contributing to differences between previous studies and the current report. The positive outcome of our specificity tests for the 3NT primary antibody supports the validity of our results. Unfortunately, the 3NT antibody used did not indicate which proteins contain nitrated tyrosine residues. Future studies are necessary to establish which specific proteins contain nitrated tyrosine in midbrain DA neurons. Indeed, protein nitration is not a ubiquitous event, but affects a subset of proteins including α-synuclein, TH, parkin, Mn-superoxide dismutase, neurofilament and tau, among others (Ischiropoulos, 2003).

Aging is associated with the accumulation of oxidative and nitrative damage; however, previous studies have not evaluated changes in midbrain DA neurons. Our data suggest that nitrative damage is a lifelong process, beginning in young animals and progressively accumulating with advancing age. The pattern of 3NT accumulation was similar to the pattern of DA neuron degeneration in PD, where vtSN DA neurons were more affected than dtSN and VTA neurons. Furthermore, our previous analysis (Kanaan *et al.*, 2007) indicates that aging in these monkeys is associated with an identical pattern of loss of TH immunoreactivity. Nitration of TH leads to a loss of TH activity in pheochromocytoma-12

cells treated with peroxynitrite or 1-methy l4-phenyl 1,2,3,6-tetrahydropyridine (Ara *et al.*, 1998). Furthermore, loss of striatal DA levels in 1-methyl 4-phenyl 1,2,3,6-tetrahydropyridine-treated mice was paralleled by increased 3NT residues in TH (Ara *et al.*, 1998). Given nitration-associated loss of TH activity, it is interesting that age-related accumulation of 3NT occurs in DA neurons that exhibit age-related reductions in TH, and that the region most affected by nitrative damage, the vtSN, exhibits the most dramatic reduction in TH levels (Kanaan *et al.*, 2007). Recently, Blanchard-Fillion *et al.* (2007) demonstrated that 3NT can reduce levels of intracellular DA and caused degeneration of pheochromocytoma-12 cells and primary rat DA neurons in culture; this appeared to be mediated by caspases and 3NT metabolism. These data suggest that age-related accumulation of 3NT in the nonhuman primate midbrain precedes reductions in the expression of the DA phenotype and may play a role in the loss of the DA phenotype.

Accumulation of nitrative damage in DA neurons of PD patients and animals models suggests a role for nitrative damage in the pathogenesis of PD (Ischiropoulos & Beckman, 2003; Jenner, 2003; Halliwell, 2006). Increased levels of nitrated α-synuclein and parkin are found in PD brains, and nitration of these proteins can interfere with their function and increase the potential for aggregation (Giasson *et al.*, 2000; Paxinou *et al.*, 2001; Chung *et al.*, 2004; Hodara *et al.*, 2004; Mishizen-Eberz *et al.*, 2005). Recently, our group has shown that soluble α-synuclein accumulates in vulnerable midbrain DA neurons during normal aging in humans and nonhuman primates, and loss of the DA phenotype (TH expression) occurs specifically in neurons that accumulate á-synuclein (Chu & Kordower, 2007). The present data provide further support for the notion that age-related changes in ventral midbrain DA neurons are important in DA neuron degeneration in PD. Moreover, the data suggest age-related accumulation of oxidative and/or nitrative damage may be involved in abnormal protein accumulation and loss of the DA phenotype.

The metabolism and/or auto-oxidation of excess cytosolic DA generates free radicals, which are believed to be involved in DA neuron degeneration (Cantuti-Castelvetri *et al.*, 2003; Hald & Lotharius, 2005). A mechanism through which DA neurons can protect against DA-derived free radical damage is repackaging cytosolic DA (recovered via DAT-mediated reuptake) back into synaptic vesicles via VMAT. The majority of our results are consistent with the hypothesis that DA neurons with increased capacity to accumulate excess cytosolic DA are more susceptible to cellular damage such as protein nitration.

Consistent with previous work (Freed *et al.*, 1995; Haber *et al.*, 1995; Miller *et al.*, 1997, 1999; Gonzalez-Hernandez *et al.*, 2004; Liang *et al.*, 2004), we found the highest levels of DAT, VMAT and the DAT/VMAT ratio in vtSN neurons. Moreover, individual DA neurons with higher DAT, VMAT and, importantly, DAT/VMAT ratios had higher levels of 3NT. It is interesting that DAT was highest in vtSN DA neurons, the DA neurons with the greatest age-related loss of TH. This may represent a compensatory response aimed at maintaining DA homeostasis. Indeed, evidence suggests post-translational modifications of DAT occur during normal aging that are aimed at maintaining DAT activity in rats (Cruz-Muros *et al.*, 2007). Higher levels of VMAT were associated with higher 3NT levels, which disagrees with the contention that higher levels of VMAT would more effectively sequester cytosolic DA and reduce exposure to free radical damage (Liang *et al.*, 2004; Caudle *et al.*, 2007). However, linear regression analyses confirmed that neurons with higher levels of DAT also had higher levels of VMAT. These results highlight the importance of evaluating the DAT/VMAT ratio on an individual cell basis. As expected, individual DA neurons with higher DAT/VMAT ratios had higher levels of 3NT damage in aged animals, despite the overall age-related reduction in DAT and DAT/VMAT ratio values. Higher levels of 3NT in aged DA neurons, and simultaneous reduction in overall DAT/VMAT ratio values, suggest there is an accumulation of 3NT damage with time. This may occur due to an increased rate of

protein damage and/or reduced ability to clear damaged proteins through proteolytic mechanisms. Further studies are necessary to elucidate the events responsible for the accumulation of protein nitration in midbrain DA neurons of aging monkeys.

We hypothesize that an underlying cycle of interconnected events influences DA neuron dysfunction and death throughout the lifetime of a normal DA neuron. Importantly, the risk factors that drive this cycle appear to be very similar between normal aging and PD, allowing aging to serve as a model for specific aspects of PD. We propose that normal aging and PD can be differentiated by the rate at which this cycle progresses. During normal aging the cycle progresses at a slow rate, which only causes DA neuron dysfunction. This translates into sustained neuronal viability but with reduced DA production and the motor abnormalities associated with normal aging. In contrast, PD occurs when the cycle is accelerated by a variety of potential events (e.g. genetic predispostion and environmental toxin exposure) occurring throughout the life of an individual. We propose that PD develops when the cascade of events accelerates to a rate at which DA neuron degeneration ensues and compensatory mechanisms are overwhelmed, eventually resulting in frank neuronal degeneration and symptomatic PD. Our hypothesis also accounts for the regional differences in susceptibility to degeneration. In vtSN DA neurons, we propose that the cycle naturally progresses at a faster rate than in resistant DA neurons located in the dtSN and VTA. The resulting greater level of cellular dysfunction in ventral tier neurons enhances their vulnerability to degeneration. Thus, we believe that accumulating evidence is consistent with the view that, at the level of cellular mechanisms, events occurring during normal aging are related to those in PD. Continued research on age-related and region-specific cellular changes provide a point of access to further our understanding of the events involved in PD.

Supplementary Material

Refer to Web version on PubMed Central for supplementary material.

Acknowledgments

We would like to express our thanks to Brian Daley for his technical assistance. This work was supported by NIH grant AG17092 (T.J.C.) and the Millennium Scholars Fund at the University of Cincinnati (T.J.C.).

Abbreviations

$^{+}$	-positive
3NT	nitrotyrosine
DA	dopamine
DAT	dopamine transporter
dtSN	substantia nigra, dorsal tier
PD	Parkinson’s disease
SN	substania nigra
TH	tyrosine hydroxylase
VMAT	vesicular monoamine transporter-2
VTA	ventral tegmental area
vtSN	substantia nigra, ventral tier

References

Alam ZI, Daniel SE, Lees AJ, Marsden DC, Jenner P, Halliwell B. A generalised increase in protein carbonyls in the brain in Parkinson's but not incidental Lewy body disease. J. Neurochem. 1997a; 69(3):1326–1329. [PubMed: 9282961]

Alam ZI, Jenner A, Daniel SE, Lees AJ, Cairns N, Marsden CD, Jenner P, Halliwell B. Oxidative DNA damage in the parkinsonian brain: an apparent selective increase in 8-hydroxyguanine levels in substantia nigra. J. Neurochem. 1997b; 69(3):1196–1203. [PubMed: 9282943]

Ara J, Przedborski S, Naini AB, Jackson-Lewis V, Trifiletti RR, Horwitz J, Ischiropoulos H. Inactivation of tyrosine hydroxylase by nitration following exposure to peroxynitrite and 1-methyl-4-phenyl-1,2,3,6-tetrahydropyridine (MPTP). Proc. Natl Acad. Sci. USA. 1998; 95(13): 7659–7663. [PubMed: 9636206]

Asanuma M, Miyazaki I, az-Corrales FJ, Ogawa N. Quinone formation as dopaminergic neuron-specific oxidative stress in the pathogenesis of sporadic Parkinson's disease and neurotoxin-induced parkinsonism. Acta Med. Okayama. 2004; 58(5):221–233. [PubMed: 15666991]

Beckman JS, Koppenol WH. Nitric oxide, superoxide, and peroxynitrite: the good, the bad, and ugly. Am. J. Physiol. 1996; 271(5 Pt 1):C1424–C1437. [PubMed: 8944624]

Blanchard-Fillion B, Prou D, Polydoro M, Spielberg D, Tsika E, Wang Z, Hazen SL, Koval M, Przedborski S, Ischiropoulos H. Metabolism of 3-nitrotyrosine induces apoptotic death in dopaminergic cells. J. Neurosci. 2007; 26(23):6124–6130. [PubMed: 16763020]

Cantuti-Castelvetri I, Shukitt-Hale B, Joseph JA. Dopamine neurotoxicity: age-dependent behavioral and histological effects. Neurobiol. Aging. 2003; 24(5):697–706. [PubMed: 12885577]

Caudle WM, Richardson JR, Wang MZ, Taylor TN, Guillot TS, McCormack AL, Colebrooke RE, Di Monte DA, Emson PC, Miller GW. Reduced vesicular storage of dopamine causes progressive nigrostriatal neurodegeneration. J. Neurosci. 2007; 27(30):8138–8148. [PubMed: 17652604]

Chu Y, Kordower JH. Age-associated increases of alpha-synuclein in monkeys and humans are associated with nigrostriatal dopamine depletion: is this the target for Parkinson's disease? Neurobiol. Dis. 2007; 25(1):134–149. [PubMed: 17055279]

Chung YH, Shin CM, Joo KM, Kim MJ, Cha CI. Immunohistochemical study on the distribution of nitrotyrosine and neuronal nitric oxide synthase in aged rat cerebellum. Brain Res. 2002; 951(2): 316–321. [PubMed: 12270511]

Chung KK, Thomas B, Li X, Pletnikova O, Troncoso JC, Marsh L, Dawson VL, Dawson TM. S-nitrosylation of parkin regulates ubiquitination and compromises parkin's protective function. Science. 2004; 304(5675):1328–1331. [PubMed: 15105460]

Cruz-Muros I, Afonso-Oramas D, Abreu P, Pérez-Delgado MM, Rodrí-guez M, González-Hernández T. Aging effects on the dopamine transporter expression and compensatory mechanisms. Neurobiol. Aging. 2007 (in press).

Damier P, Hirsch EC, Agid Y, Graybiel AM. The substantia nigra of the human brain. II. Patterns of loss of dopamine-containing neurons in Parkinson's disease. Brain. 1999; 122(Pt 8):1437–1448. [PubMed: 10430830]

Del Moral ML, Esteban FJ, Hernandez R, Blanco S, Molina FJ, Martinez-Lara E, Siles E, Viedma G, Ruiz A, Pedrosa JA, Peinado MA. Immunohistochemistry of neuronal nitric oxide synthase and protein nitration in the striatum of the aged rat. Microsc. Res. Tech. 2004; 64(4):304–311. [PubMed: 15481048]

Duda JE, Giasson BI, Chen Q, Gur TL, Hurtig HI, Stern MB, Gollomp SM, Ischiropoulos H, Lee VM, Trojanowski JQ. Widespread nitration of pathological inclusions in neurodegenerative synucleinopathies. Am. J. Pathol. 2000; 157(5):1439–1445. [PubMed: 11073803]

Ferrante RJ, Hantraye P, Brouillet E, Beal MF. Increased nitrotyrosine immunoreactivity in substantia nigra neurons in MPTP treated baboons is blocked by inhibition of neuronal nitric oxide synthase. Brain Res. 1999; 823(1–2):177–182. [PubMed: 10095024]

Floor E, Wetzel MG. Increased protein oxidation in human substantia nigra pars compacta in comparison with basal ganglia and prefrontal cortex measured with an improved dinitrophenylhydrazine assay. J. Neurochem. 1998; 70(1):268–275. [PubMed: 9422371]

Freed C, Revay R, Vaughan RA, Kriek E, Grant S, Uhl GR, Kuhar MJ. Dopamine transporter immunoreactivity in rat brain. J. Comp. Neurol. 1995; 359(2):340–349. [PubMed: 7499533]

Giasson BI, Duda JE, Murray IV, Chen Q, Souza JM, Hurtig HI, Ischiropoulos H, Trojanowski JQ, Lee VM. Oxidative damage linked to neurodegeneration by selective alpha-synuclein nitration in synucleinopathy lesions. Science. 2000; 290:985–989. [PubMed: 11062131]

Gibb WR, Lees AJ. Anatomy, pigmentation, ventral and dorsal subpopulations of the substantia nigra, and differential cell death in Parkinson's disease. J. Neurol. Neurosurg. Psychiatry. 1991; 54(5): 388–396. [PubMed: 1865199]

Gonzalez-Hernandez T, Barroso-Chinea P, De La Cruz Muros I, Mar Perez-Delgado M, Rodriguez M. Expression of dopamine and vesicular monoamine transporters and differential vulnerability of mesostriatal dopaminergic neurons. J. Comp. Neurol. 2004; 479(2):198–215. [PubMed: 15452855]

Gundersen HJ, Jensen EB, Kieu K, Nielsen J. The efficiency of systematic sampling in stereology – reconsidered. J. Microsc. 1999; 193(Pt 3):199–211. [PubMed: 10348656]

Haber SN, Ryoo H, Cox C, Lu W. Subsets of midbrain dopaminergic neurons in monkeys are distinguished by different levels of mRNA for the dopamine transporter: comparison with the mRNA for the D2 receptor, tyrosine hydroxylase and calbindin immunoreactivity. J. Comp. Neurol. 1995; 362(3):400–410. [PubMed: 8576447]

Hald A, Lotharius J. Oxidative stress and inflammation in Parkinson's disease: is there a causal link? Exp. Neurol. 2005; 193(2):279–290. [PubMed: 15869932]

Halliwell B. Oxidative stress and neurodegeneration: where are we now? J. Neurochem. 2006; 97(6): 1634–1658. [PubMed: 16805774]

Hodara R, Norris EH, Giasson BI, Mishizen-Eberz AJ, Lynch DR, Lee VM, Ischiropoulos H. Functional consequences of alpha-synuclein tyrosine nitration: diminished binding to lipid vesicles and increased fibril formation. J. Biol. Chem. 2004; 279(46):47746–47753. [PubMed: 15364911]

Ischiropoulos H. Biological selectivity and functional aspects of protein tyrosine nitration. Biochem. Biophys. Res. Commun. 2003; 305(3):776–783. [PubMed: 12763060]

Ischiropoulos H, Beckman JS. Oxidative stress and nitration in neurodegeneration: cause, effect, or association? J. Clin. Invest. 2003; 111(2):163–169. [PubMed: 12531868]

Jenner P. Oxidative stress in Parkinson's disease. Ann. Neurol. 2003; 53(Suppl. 3):S26–S36. [PubMed: 12666096]

Kanaan NM, Collier TJ, Marchionini DM, McGuire SO, Fleming MF, Sortwell CE. Exogenous erythropoietin provides neuroprotection of grafted dopamine neurons in a rodent model of Parkinson's disease. Brain Res. 2006; 1068(1):221–229. [PubMed: 16368081]

Kanaan NM, Kordower JH, Collier TJ. Age-related accumulation of Marinesco bodies and lipofuscin in rhesus monkey midbrain dopamine neurons: Relevance to selective neuronal vulnerability. J. Comp. Neurol. 2007; 502(5):683–700. [PubMed: 17436290]

Liang CL, Nelson O, Yazdani U, Pasbakhsh P, German DC. Inverse relationship between the contents of neuromelanin pigment and the vesicular monoamine transporter-2: human midbrain dopamine neurons. J. Comp. Neurol. 2004; 473(1):97–106. [PubMed: 15067721]

Miller GW, Staley JK, Heilman CJ, Perez JT, Mash DC, Rye DB, Levey AI. Immunochemical analysis of dopamine transporter protein in Parkinson's disease. Ann. Neurol. 1997; 41(4):530–539. [PubMed: 9124811]

Miller GW, Gainetdinov RR, Levey AI, Caron MG. Dopamine transporters and neuronal injury. Trends Pharmacol. Sci. 1999; 20(10):424–429. [PubMed: 10498956]

Mishizen-Eberz AJ, Norris EH, Giasson BI, Hodara R, Ischiropoulos H, Lee VM, Trojanowski JQ, Lynch DR. Cleavage of alpha-synuclein by calpain: potential role in degradation of fibrillized and nitrated species of alpha-synuclein. Biochemistry. 2005; 44(21):7818–7829. [PubMed: 15909996]

Paxinou E, Chen Q, Weisse M, Giasson BI, Norris EH, Rueter SM, Trojanowski JQ, Lee VM, Ischiropoulos H. Induction of alpha-synuclein aggregation by intracellular nitrative insult. J. Neurosci. 2001; 21(20):8053–8061. [PubMed: 11588178]

Reynolds MR, Berry RW, Binder LI. Nitration in neurodegeneration: deciphering the "Hows" "nYs". Biochemistry. 2007; 46(25):7325–7336. [PubMed: 17542619]

Salvemini D, Doyle TM, Cuzzocrea S. Superoxide, peroxynitrite and oxidative/nitrative stress in inflammation. Biochem. Soc. Trans. 2006; 34(Pt 5):965–970. [PubMed: 17052238]

Shin CM, Chung YH, Kim MJ, Lee EY, Kim EG, Cha CI. Age-related changes in the distribution of nitrotyrosine in the cerebral cortex and hippocampus of rats. Brain Res. 2002; 931(2):194–199. [PubMed: 11897106]

Sloane JA, Hollander W, Moss MB, Rosene DL, Abraham CR. Increased microglial activation and protein nitration in white matter of the aging monkey. Neurobiol. Aging. 1999; 20(4):395–405. [PubMed: 10604432]

Squier TC. Oxidative stress and protein aggregation during biological aging. Exp. Gerontol. 2001; 36(9):1539–1550. [PubMed: 11525876]

Torreilles F, Salman-Tabcheh S, Guerin M, Torreilles J. Neurodegenerative disorders: the role of peroxynitrite. Brain Res. Brain Res. Rev. 1999; 30(2):153–163. [PubMed: 10525172]

Uttenthal LO, Alonso D, Fernandez AP, Campbell RO, Moro MA, Leza JC, Lizasoain I, Esteban FJ, Barroso JB, Valderrama R, Pedrosa JA, Peinado MA, Serrano J, Richart A, Bentura ML, Santacana M, Martinez-Murillo R, Rodrigo J. Neuronal and inducible nitric oxide synthase and nitrotyrosine immunoreactivities in the cerebral cortex of the aging rat. Microsc. Res. Tech. 1998; 43(1):75–88. [PubMed: 9829462]

West MJ, Gundersen HJ. Unbiased stereological estimation of the number of neurons in the human hippocampus. J. Comp. Neurol. 1990; 296(1):1–22. [PubMed: 2358525]

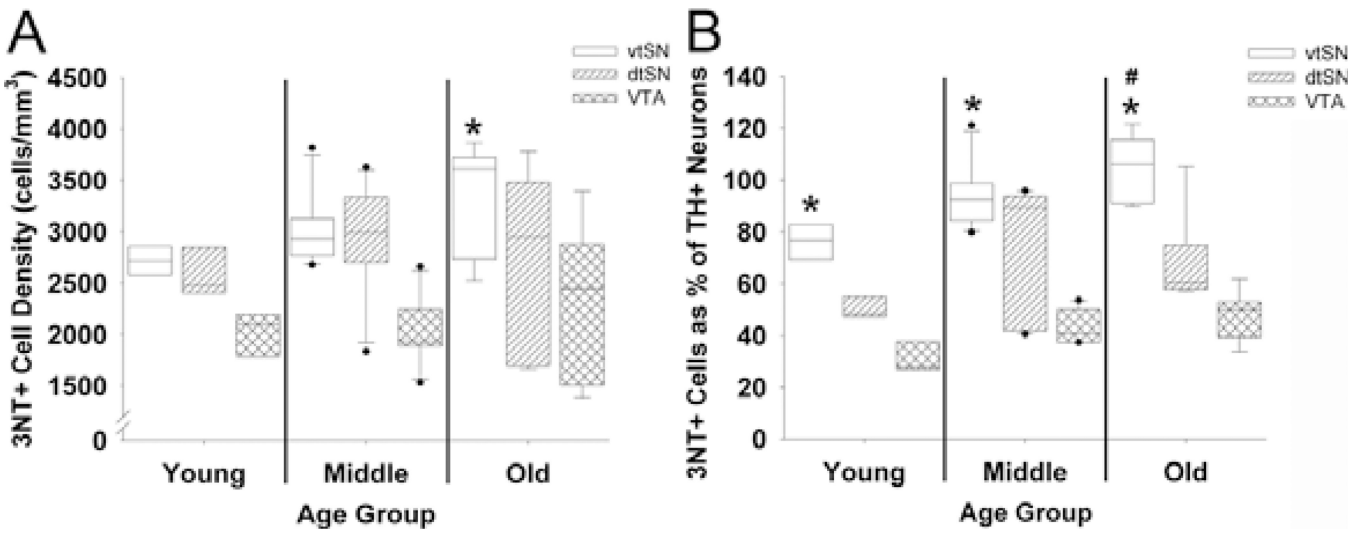

Fig. 1.

Advancing chronological age was associated with increases in the percentage of DA neurons containing 3NT, and the vtSN had more DA neurons containing 3NT than did the VTA. (A) $3NT^+$ neuron density was significantly greater in the vtSN than in the VTA of old animals ($^*P < 0.05$). The number of $3NT^+$ neurons did not change with advancing age in the vtSN, dtSN or VTA. (B) The percentage of TH^+ neurons containing 3NT was significantly increased in old animals compared to young animals ($^{\#}P < 0.05$). In young, middle-aged and old animals the proportion of vtSN TH^+ neurons containing 3NT was significantly greater than the proportion in the VTA ($^*P < 0.05$).

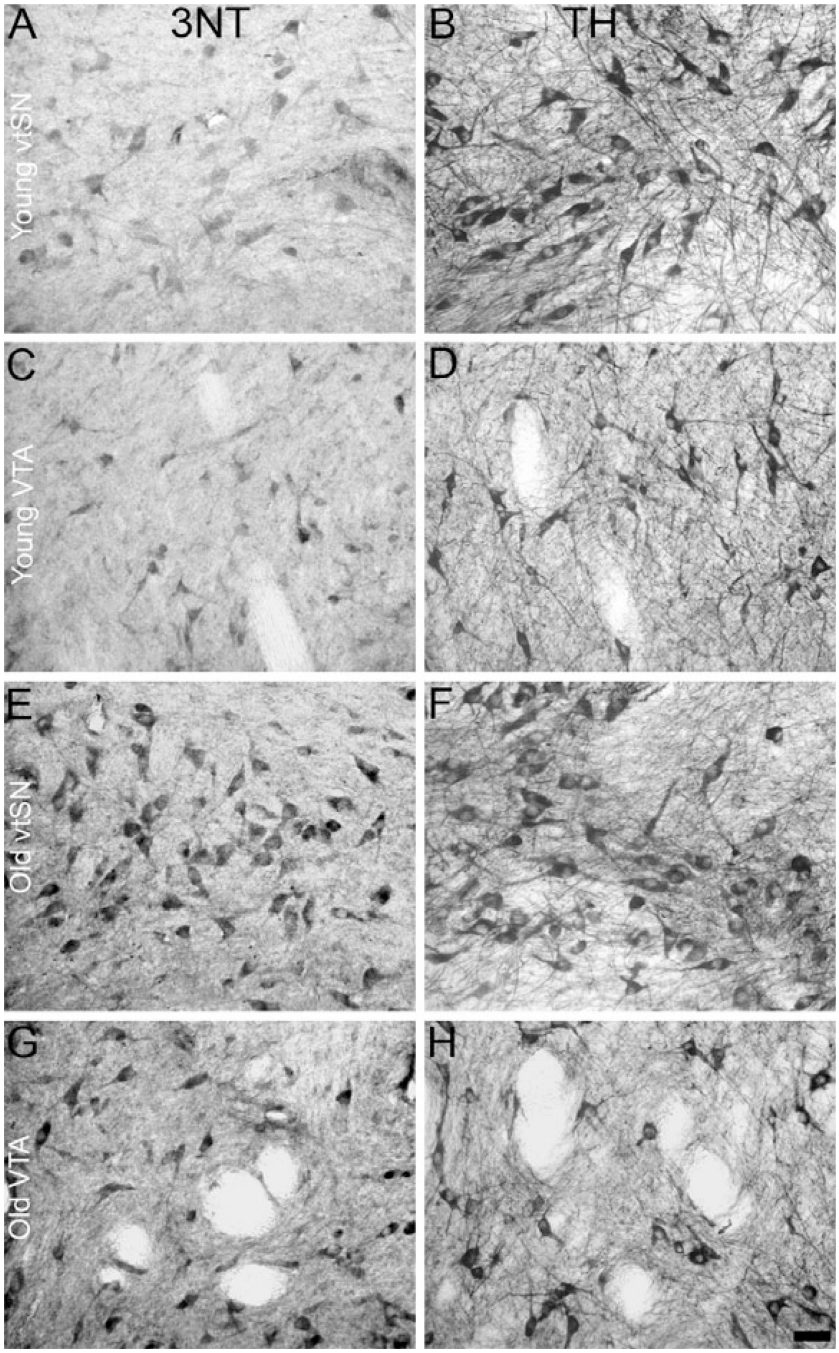

Fig. 2.

Comparisons between 3NT and TH immunohistochemistry demonstrate that $3NT^+$ neurons in the midbrain were mostly DA neurons, and there was an age-related increase in the percentage of DA neurons containing 3NT. (A vs. B, C vs. D, E vs. F and G vs. H) Visually comparing 3NT staining to TH staining clearly illustrates the similarities between neurons labeled with these markers. This suggests the vast majority of $3NT^+$ neurons in the vtSN, dtSN and VTA were DA neurons. In the vtSN (A and B compared to E and F) and VTA (C and D compared to G and H), the proportion of $3NT^+$ TH neurons was significantly greater in the old animals (E and F, and G and H) than in the young animals (A and B, and C and D). In young (A and B compared to C and D) and old animals (E and F compared to G and

H), the proportion of $3NT^+$ TH neurons was significantly greater in the vtSN (A and B, and E and F) than in the VTA (C and D, and G and H). Scale bar, 50 μm in H (applies to A–H).

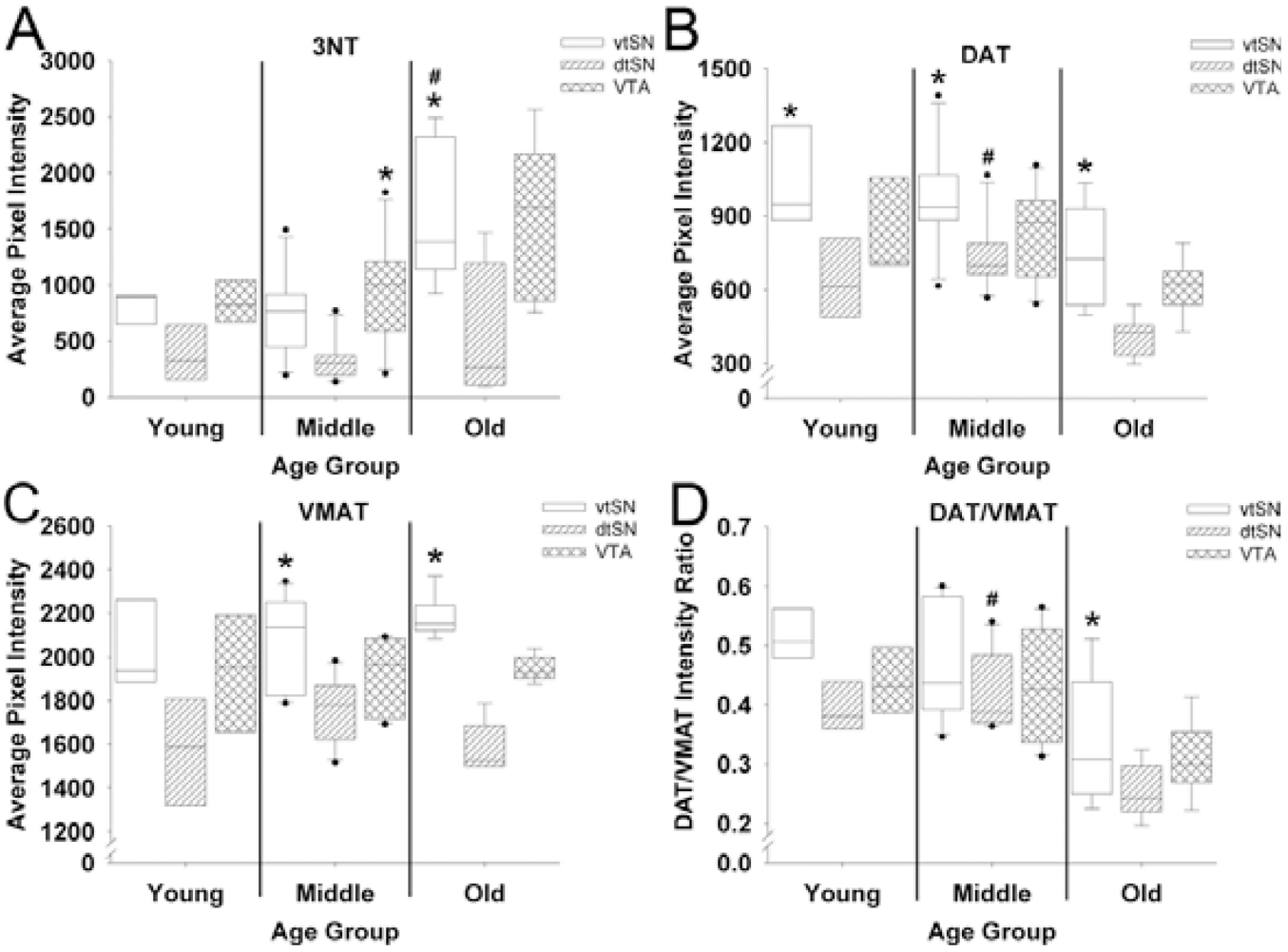

Fig. 3.

Immunofluorescence intensity for 3NT, DAT, VMAT and DAT/VMAT in midbrain DA neurons. (A) Only in the vtSN was there a significant increase in 3NT fluorescence intensity in old animals compared to young animals ($^{\#}P < 0.05$). In young animals, all three DA subregions had similar levels of 3NT immunofluorescence. By contrast, VTA neurons in middle-aged animals and vtSN neurons in old animals had significantly greater levels of 3NT immunofluorescence than dtSN neurons ($^{*}P < 0.05$ vs. dtSN). (B) In the vtSN and VTA, DAT did not change with age; however, DAT intensity was greater in middle-aged animals than in old animals ($^{\#}P < 0.05$). In all three age groups, DAT intensity was greatest in vtSN DA neurons, reaching statistical significance when compared to the dtSN ($^{*}P < 0.05$ vs. dtSN). (C) No age-related changes were detected in VMAT intensity. In young animals, the DA neurons in all three midbrain subregions had similar VMAT intensity. In middle-aged and old animals, the level of VMAT intensity was greatest in vtSN DA neurons, reaching statistical significance compared to the dtSN ($^{*}P < 0.05$ vs. dtSN). (D) In the vtSN and VTA, the DAT/VMAT ratio did not change with age; however, the DAT/VMAT ratio was greater in middle-aged animals than in old animals ($^{\#}P < 0.05$). In young and middle-aged animals, the DAT/VMAT ratio was similar between DAergic subregions; however, in aged animals the DAT/VMAT ratio was significantly greater in vtSN DA neurons than in the dtSN ($^{*}P < 0.05$ vs. dtSN).

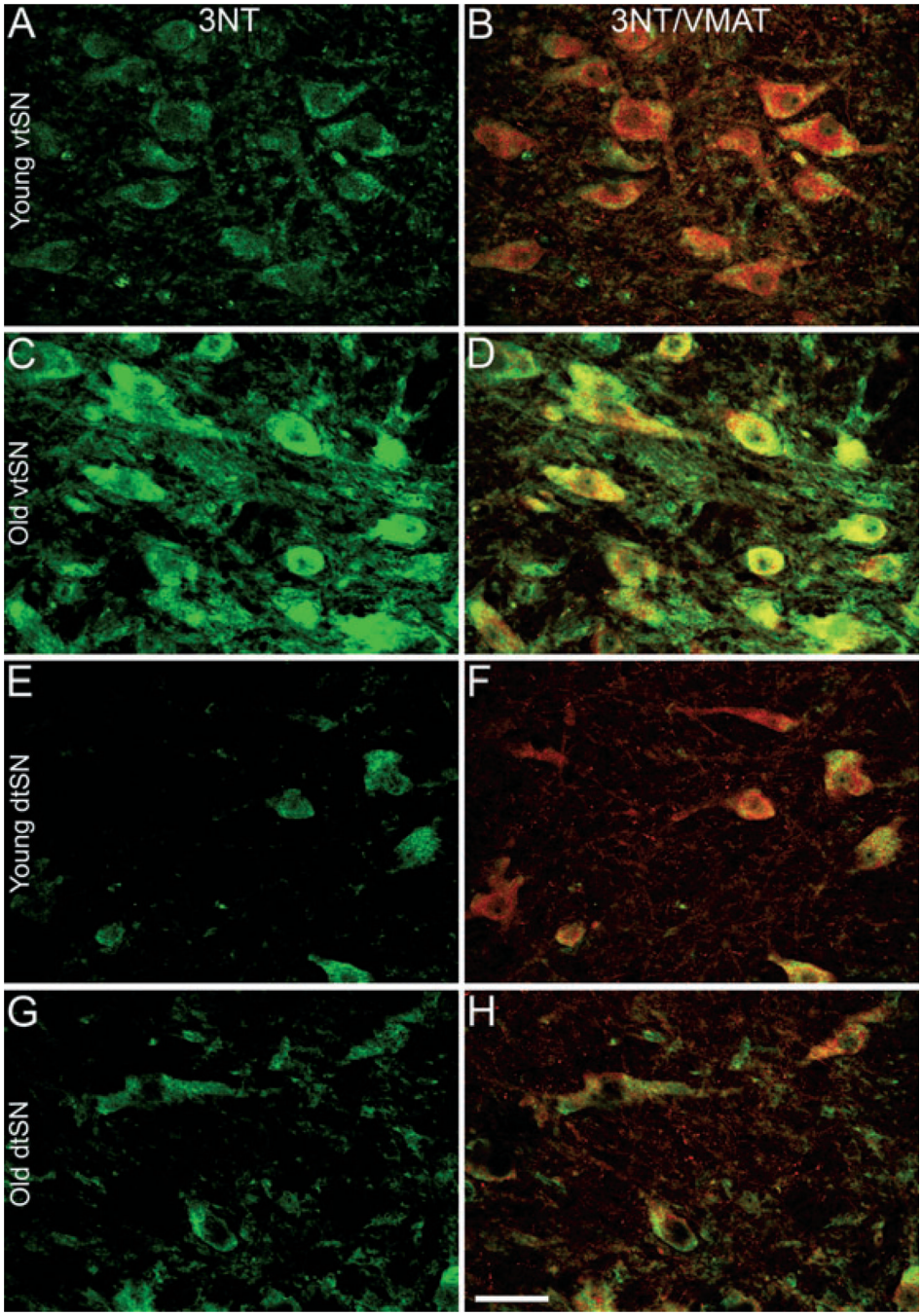

Fig. 4.

Aging was associated with increased intensity of 3NT immunofluorescence in vtSN DA neurons, and the intensity in vtSN DA neurons was greater than the intensity of dtSN DA neurons. (A, B, C and D) In the vtSN, the intensity of 3NT (green; A and C) in DA neurons ($VMAT^+$ neurons: red in B, and D) of (C) aged animals was significantly greater than those in (A) young animals. (E, F, G and H) In the dtSN, there was not a significant change in the intensity of 3NT immunofluorescence with advancing age (E, young; G, old). In aged animals, the intensity of 3NT in vtSN neurons was greater than the intensity of neurons in the dtSN (compare C and G). In contrast, the intensity of 3NT was statistically similar in all three DAergic subregions of young animals [compare (A) vtSN to (E) dtSN]. (B, D, F and

H) The co-localization (yellow) of VMAT (red) with 3NT (green) is shown to confirm that $3NT^+$ neurons were DAergic. Scale bar, 50 μm in H (applies to A–H).

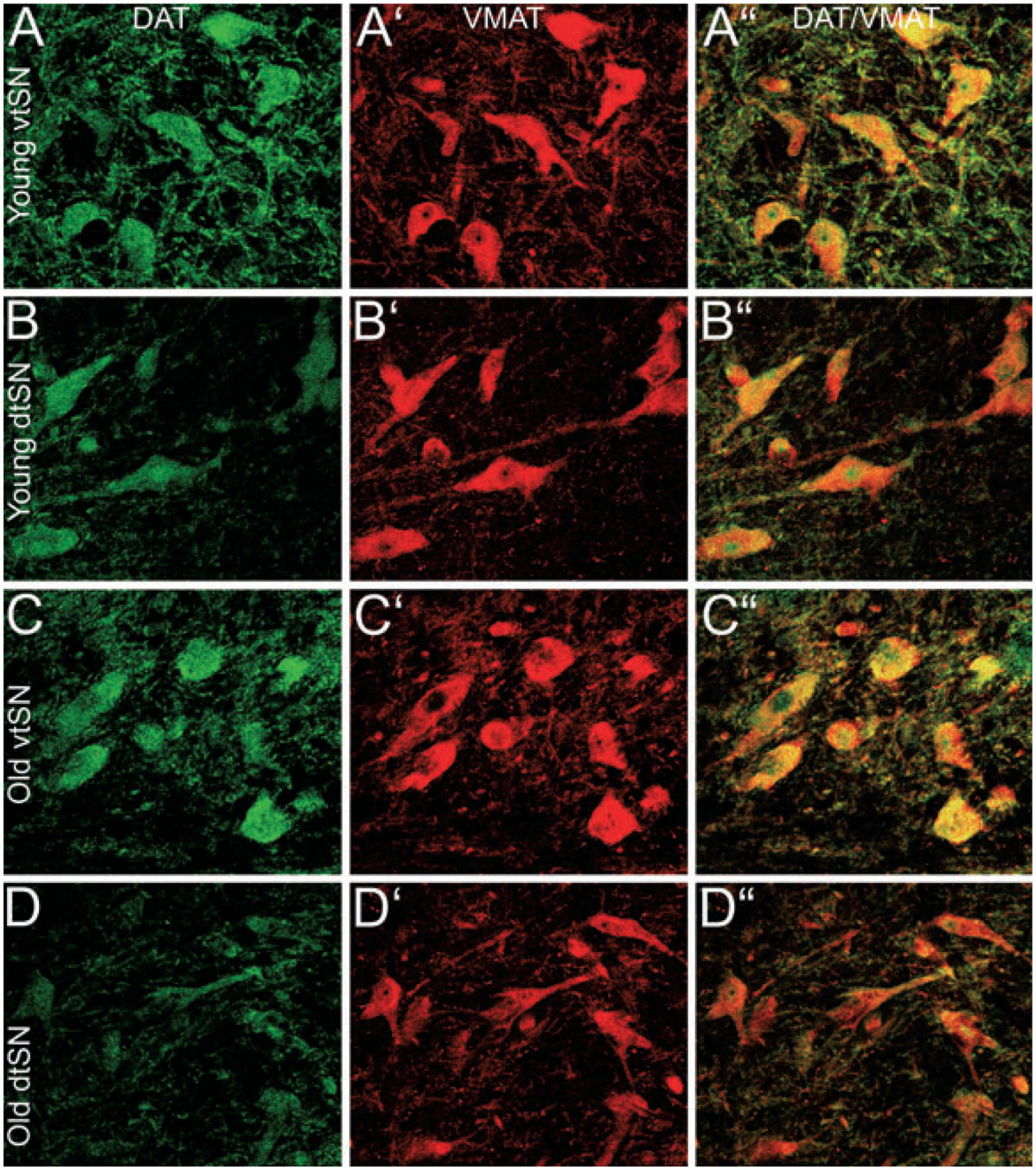

Fig. 5.

In midbrain DA neurons, DAT intensity decreased with age in the dtSN, VMAT intensity remained unchanged with age, and the intensity of both transporters was greater in the vtSN than in the dtSN. (A, B, C and D) In the vtSN, DAT intensity was similar in (A) young and (C) old DA neurons. In the dtSN, increasing age was significantly correlated with reductions in the level of DAT immunofluorescence [(B) young and (D) old]. Regional comparisons show that the level of DAT was greater in vtSN DA neurons than in dtSN DA neurons in all age groups (compare A to B and C to D). (A′, B′, C′ and D′) The level of VMAT immunofluorescence was unchanged in all DAergic subregions during normal aging (compare A′ to C′ for vtSN and B′ to D′ for dtSN). The level of VMAT

immunofluorescence was similar between DAergic subregions of young animals (compare A′ for vtSN with B′ for dtSN). However, VMAT intensity was greater in (C′) vtSN neurons than in (D′) dtSN neurons in old animals. (A″, B″, C″ and D″) Merged images of DAT (green) and VMAT (red) immunofluorescence confirm the co-localization (yellow) of the two markers in DAergic neurons of the midbrain. Scale bar, 50 μm in D″ (applies to A–D″).

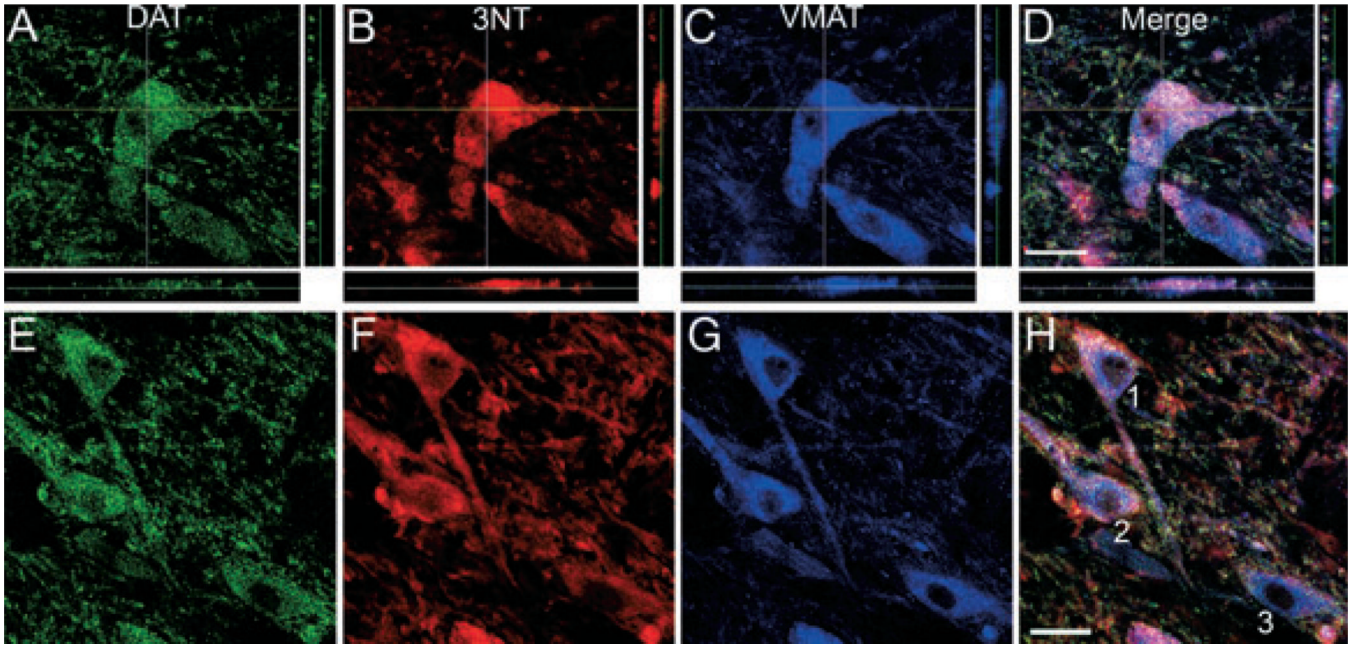

Fig. 6.

Higher levels of DAT, VMAT and DAT/VMAT ratios were associated with higher 3NT levels in midbrain DA neurons. (A–D) The co-localization of 3NT (red, B) with DAT (green, A) and VMAT (blue, C) was confirmed using confocal microscopy. Analysis through the *z*-plane in a confocal *z*-stack clearly illustrates the co-localization of 3NT in midbrain DA neurons (A–D). (E–H) Linear regression models demonstrate that DAT (green, E), VMAT (blue, G) and DAT/VMAT levels were significant predictors for the level of 3NT (red, F) in individual DA neurons. In addition, the level of DAT, VMAT and DAT/VMAT ratios was positively correlated with 3NT levels. The relationship between DA transporter intensity and 3NT intensity are illustrated in the representative DA neurons in E–H. Neuron 1: DAT = 616, VMAT = 1019, DAT/VMAT ratio = 0.60, 3NT = 1580; Neuron 2: DAT = 636, VMAT = 1111, DAT/VMAT ratio = 0.57, 3NT = 1344; Neuron 3: DAT = 447, VMAT = 869, DAT/VMAT ratio = 0.51, 3NT = 742. All images are from the vtSN of an aged animal. Scale bars, 25 μm in D (applies to A–D) and H (applies to E–H).